dipole–dipole interaction (Bolton, 1964). It might be important in the multiple pharmacological effect that each phenobarbital molecule is surrounded by four theophylline molecules with N—H · · · N and C—H · · · O hydrogen bonds.

References

BENDER, M. & NELSON, J. A. (1973). *J. Chem. Soc. Faraday* I, **69**, 2074–2079.
BOLTON, W. (1964). *Nature, Lond.* **201**, 987–989.
CRAVEN, B. M. & GARTLAND, G. L. (1974). *Acta Cryst.* B**30**, 1191–1195.
GARTLAND, G. L., GATEHOUSE, B. M. & CRAVEN, B. M. (1975). *Acta Cryst.* B**31**, 203–211.
GERMAIN, G., MAIN, P. & WOOLFSON, M. M. (1971). *Acta Cryst.* A**27**, 368–376.

HIGGINS, W. M. & DUNKER, M. F. W. (1944). *J. Amer. Pharm. Assoc. Sci. Ed.* **33**, 310–314.
International Tables for X-ray Crystallography (1962). Vol. III, pp. 202–203. Birmingham: Kynoch Press.
KIM, S. H. & RICH, A. (1968). *Proc. Natl. Acad. Sci. US*, **60**, 402–408.
KISTENMACHER, T. J. (1975). *Acta Cryst.* B**31**, 85–89.
KISTENMACHER, T. J. & SZALDA, D. J. (1975). *Acta Cryst.* B**31**, 90–96.
SHEFTER, E. (1969). *J. Pharm. Sci.* **58**, 710–714.
SHIEH, H. S. & VOET, D. (1975). *Acta Cryst.* B**31**, 2192–2201.
SUTOR, D. J. (1958). *Acta Cryst.* **11**, 83–87.
UNICS (1973). *The Universal Crystallographic Computing System*. Library programs in the Computation Center of Osaka Univ.
VOET, D. (1971). *Amer. Cryst. Assoc. Abs. Pap.* p. 74.
VOET, D. (1972). *J. Amer. Chem. Soc.* **94**, 8213–8222.
VOET, D. & RICH, A. (1972). *J. Amer. Chem. Soc.* **94**, 5888–5891.

The Crystal Structure of (−)589-Oxalatobis(ethylenediamine)cobalt(III) (+)589-Dicyanomalonatodiamminecobaltate(III) Trihydrate

BY K. TORIUMI, S. SATO AND Y. SAITO

The Institute for Solid State Physics, The University of Tokyo, Roppongi-7, Minato-ku, Tokyo 106, Japan

(−)589-[Co(ox)(en)2] (+)589-[Co(CN)2(mal)(NH3)2].3H2O crystallizes in the orthorhombic space group $P2_12_12_1$ with $a = 16.709$ (1), $b = 18.139$ (1), $c = 7.569$ (1) Å and $Z = 4$. The structure was refined by least-squares calculations to give an R value of 0.034 for 3304 observed amplitudes. The complex anion is a *cis–cis* isomer: a Co atom is surrounded nearly octahedrally by two C atoms of cyano groups, two N atoms of ammonia molecules, both in *cis* positions, and two O atoms of a malonato group. The absolute configuration of the complex anion, (+)589-[Co(CN)2(mal)(NH3)2]−, can be designated as Δ, provided that the chirality is defined by the line joining the two C atoms of the cyano groups and that joining the two N atoms of the ammonia molecules. During the data collection, some strong reflexions with low diffraction angles strikingly increased their intensities. The increase in intensity may be ascribed to a change in the extinction effect under X-irradiation.

Introduction

Seven optically active complexes of Co^III were isolated whose optical activity arises from the chiral configuration of monodentates coordinated to the central Co atom (Ito & Shibata, 1976). The absolute configuration of the complex ion is of particular importance since no empirical relation between the circular dichroism spectra and the absolute configuration of such complexes has been established. The absolute configuration of one of these complexes, (−)589-[Co(NO2)2(ox)(NH3)2]−, was determined by X-ray methods (Shin-tani, Sato & Saito, 1976). In this paper, the absolute configuration of the title compound will be described.

Experimental

Crystals of (−)589-[Co(ox)(en)2] (+)589-[Co(CN)2(mal)(NH3)2].3H2O were kindly supplied by Professor M. Shibata of Kanazawa University. They are orange-red square prisms. Unit-cell dimensions were determined from Weissenberg photographs and refined on a diffractometer. The intensities of the reflexions were

measured on a Rigaku automated four-circle diffractometer using Mo $K\alpha$ radiation monochromated by a graphite plate. A crystal of dimensions $0.31 \times 0.26 \times 0.36$ mm was sealed in a thin-walled Lindemann-glass capillary with a small piece of wet filter paper to prevent loss of water of hydration, and used for intensity measurement. Of 3808 reflexions measured within the range $2\theta \leq 60°$, 3304 independent reflexions with $|F_o| \geq 3\sigma(F_o)$ were regarded as 'observed'. Corrections for Lorentz and polarization effects were applied to the data (hereafter called data set 1). During the period of the collection of data set 1 (7 d), the intensities of two standard reflexions (430, 002) increased by about 50%. At the final stage of data collection, 165 strong, low-angle reflexions were remeasured (hereafter called data set 2). The intensities of 72 very strong, low-angle reflexions in data set 2 were stronger than those of the corresponding ones in data set 1, but the remaining 93 reflexions had intensities that changed little. The maximum rate of increase of intensity was as large as 70%. It turned out at a later stage of the refinement that this phenomenon could be ascribed to the change in the extinction effect. It will be discussed later in some detail.

Crystal data are: $[CoC_6H_{16}N_4O_4][CoC_5H_8N_4O_4].3H_2O$, FW 568·27, orthorhombic, $P2_12_12_1$, $Z = 4$, $a = 16·709$ (1), $b = 18·139$ (1), $c = 7·569$ (1) Å, $U = 2293·9$ (2) Å³, $D_x = 1·65$, $D_m = 1·67$ g cm⁻³, $\mu(Mo~K\alpha) = 15·08$ cm⁻¹.

Structure determination and refinement

The structure was solved by Patterson and Fourier techniques. Block-diagonal least-squares refinement in-

Table 1. *Determination of the absolute configuration*

h k l	$|F_c(hkl)|^2$	Observed	$|F_c(hk\bar{l})|^2$
1 4 1	1544	>	807
1 7 1	824	<	1781
2 6 1	392	>	52
2,10,1	961	<	1806
4,13,1	1498	>	949
6 3 1	566	<	1005
2 4 2	1204	<	2590
3,13,2	303	<	543
4 1 3	724	>	310
2,13,3	404	<	1037
3,15,3	692	<	1260

Fig. 1. A projection of the structure along c.

$(-)_{589}\text{-[Co(ox)(en)}_2]$ $(+)_{589}\text{-[Co(CN)}_2\text{(mal)(NH}_3)_2]\cdot 3\text{H}_2\text{O}$
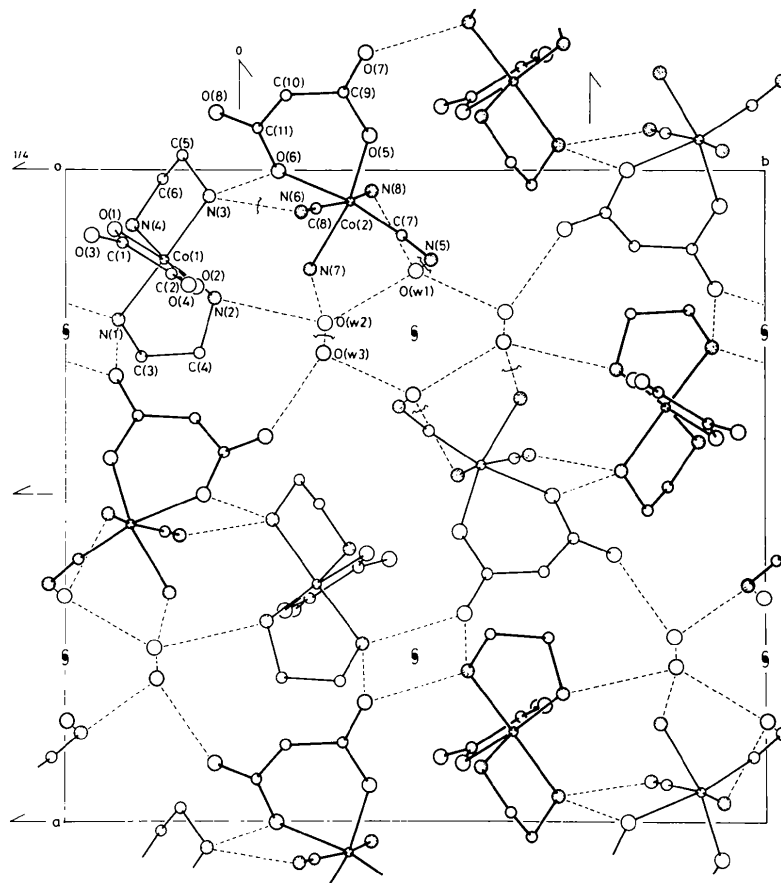
cluding H atoms, except those of the water molecules, and using data set 1 converged to an R value of 0·052. At this stage many $|F_o|$'s of very strong, low-angle reflexions were less than the calculated values, while the corresponding $|F_o|$'s in data set 2 were all closer to the $|F_c|$'s. Therefore, 72 strong, low-angle intensities of data set 1 were replaced by those of data set 2. Then a difference synthesis was calculated and the positions of the H atoms of the water molecules could be deter-mined. After inclusion of the H atoms of the water molecules, a final set of least-squares calculations was carried out with isotropic thermal parameters assumed for the H atoms. The final R value was 0·034 for the 3304 observed reflexions. Unit weight was given to all the reflexions. The scattering factors of the atoms, ex-cept H, were taken from *International Tables for X-ray Crystallography* (1962). For H the values given by Stewart, Davidson & Simpson (1965) were used.

Table 2. *Atomic parameters*

Positional parameters for non-hydrogen atoms are × 10⁴. The U_{ij}'s are defined by: $\exp[-2\pi^2(U_{11}h^2a^{*2} + \cdots + 2U_{12}hka^*b^* + \cdots) \times 10^{-3}]$. Positional parameters for the hydrogen atoms are × 10³. The isotropic temperature factor is defined by: $\exp[-8\pi^2U(\sin\theta/\lambda)^2]$. Mean value of U for the hydrogen atoms is 0·05 (2) Å².

	x	y	z	U_{11}	U_{22}	U_{33}	U_{12}	U_{13}	U_{23}
Co(1)	1370 (0)	1415 (0)	688 (1)	24 (0)	15 (0)	10 (0)	0 (0)	0 (0)	0 (0)
Co(2)	478 (0)	3946 (0)	4827 (1)	20 (0)	18 (0)	27 (0)	0 (0)	3 (0)	0 (0)
O(1)	913 (2)	704 (2)	2277 (4)	41 (2)	22 (1)	16 (1)	−8 (1)	2 (1)	1 (1)
O(2)	1799 (2)	1877 (2)	2736 (4)	32 (2)	23 (1)	15 (1)	−2 (1)	−3 (1)	−1 (1)
O(3)	1012 (3)	384 (2)	5101 (5)	81 (3)	32 (2)	22 (2)	−9 (2)	6 (2)	6 (2)
O(4)	1751 (2)	1763 (2)	5668 (5)	58 (2)	52 (2)	16 (1)	−12 (2)	−2 (2)	−8 (2)
C(1)	1133 (3)	807 (2)	3873 (6)	41 (3)	24 (2)	16 (2)	1 (2)	6 (2)	0 (2)
C(2)	1604 (3)	1537 (2)	4157 (6)	33 (2)	25 (2)	15 (2)	2 (2)	−1 (2)	−2 (2)
N(1)	2309 (2)	774 (2)	432 (5)	27 (2)	21 (2)	24 (2)	4 (1)	1 (2)	2 (1)
N(2)	1958 (2)	2120 (2)	−752 (5)	30 (2)	19 (1)	18 (2)	−1 (1)	−1 (2)	0 (1)
N(3)	418 (2)	2037 (2)	864 (5)	29 (2)	23 (2)	25 (2)	4 (2)	1 (2)	−3 (2)
N(4)	840 (2)	952 (2)	−1325 (5)	29 (2)	19 (2)	15 (1)	−2 (1)	−1 (1)	−2 (1)
C(3)	2855 (3)	1090 (3)	−914 (7)	34 (2)	37 (2)	40 (3)	10 (2)	16 (2)	9 (3)
C(4)	2820 (3)	1924 (3)	−711 (8)	28 (2)	33 (2)	40 (3)	−3 (2)	7 (2)	10 (2)
C(5)	−229 (3)	1701 (3)	−199 (7)	25 (2)	43 (3)	33 (3)	2 (2)	−2 (2)	−7 (2)
C(6)	150 (3)	1410 (3)	−1880 (6)	28 (2)	33 (2)	23 (2)	0 (2)	−5 (2)	−2 (2)
C(7)	1007 (3)	4792 (2)	5638 (8)	26 (2)	23 (2)	44 (3)	0 (2)	2 (2)	−1 (2)
C(8)	588 (3)	3579 (3)	7165 (7)	25 (2)	23 (2)	37 (2)	0 (2)	0 (2)	3 (2)
N(5)	1340 (3)	5288 (2)	6188 (8)	36 (2)	29 (2)	76 (4)	−5 (2)	−3 (3)	−5 (2)
N(6)	628 (3)	3373 (3)	8567 (7)	54 (3)	35 (2)	· 43 (3)	−2 (2)	−6 (2)	12 (2)
O(5)	−544 (2)	4368 (2)	5391 (4)	23 (1)	18 (1)	36 (2)	1 (1)	6 (1)	1 (1)
O(6)	−2 (2)	3051 (2)	3937 (5)	28 (2)	25 (2)	39 (2)	−6 (1)	9 (2)	−12 (1)
O(7)	−1812 (2)	4333 (2)	6108 (5)	24 (1)	28 (2)	45 (2)	6 (1)	12 (2)	4 (2)
O(8)	−895 (2)	2178 (2)	3843 (6)	43 (2)	28 (2)	64 (3)	−13 (2)	9 (2)	−19 (2)
C(9)	−1179 (2)	4011 (2)	5780 (6)	23 (2)	23 (2)	22 (2)	0 (2)	5 (2)	−1 (2)
C(10)	−1159 (3)	3166 (2)	5852 (7)	28 (2)	20 (2)	40 (3)	−1 (2)	10 (2)	2 (2)
C(11)	−660 (3)	2778 (2)	4457 (7)	25 (2)	23 (2)	33 (2)	0 (2)	−3 (2)	−2 (2)
N(7)	1499 (2)	3509 (2)	4137 (6)	24 (2)	30 (2)	45 (2)	2 (2)	6 (2)	−4 (2)
N(8)	323 (3)	4380 (2)	2433 (6)	38 (2)	36 (2)	27 (2)	2 (2)	2 (2)	5 (2)
O(w1)	1552 (3)	5032 (3)	106 (7)	66 (3)	56 (2)	64 (3)	−10 (2)	0 (3)	−1 (3)
O(w2)	2370 (3)	3714 (2)	417 (8)	51 (2)	40 (2)	87 (4)	−11 (2)	−13 (3)	−5 (3)
O(w3)	2824 (3)	3695 (3)	6644 (6)	47 (2)	54 (3)	57 (3)	17 (2)	−1 (2)	−2 (2)

	x	y	z		x	y	z
H(1)	206 (4)	23 (4)	50 (11)	H(16)	334 (4)	91 (3)	−99 (9)
H(2)	256 (4)	66 (4)	204 (10)	H(17)	310 (3)	220 (3)	−202 (7)
H(3)	197 (4)	245 (3)	−44 (9)	H(18)	303 (4)	209 (3)	91 (9)
H(4)	184 (3)	218 (3)	−217 (8)	H(19)	−68 (3)	212 (3)	−53 (8)
H(5)	32 (3)	216 (3)	235 (8)	H(20)	−39 (4)	140 (3)	90 (9)
H(6)	57 (3)	244 (3)	76 (8)	H(21)	−25 (3)	104 (3)	−249 (7)
H(7)	114 (3)	79 (2)	−238 (6)	H(22)	36 (3)	187 (3)	−257 (7)
H(8)	62 (3)	45 (3)	−132 (8)	H(23)	−90 (3)	297 (3)	728 (7)
H(9)	171 (3)	363 (3)	288 (8)	H(24)	−165 (4)	293 (3)	667 (9)
H(10)	146 (4)	296 (4)	360 (10)	H(25)	172 (4)	506 (4)	−158 (11)
H(11)	188 (4)	359 (3)	489 (9)	H(26)	174 (4)	531 (4)	96 (11)
H(12)	77 (3)	475 (3)	218 (8)	H(27)	278 (4)	398 (4)	125 (11)
H(13)	23 (3)	416 (3)	202 (8)	H(28)	208 (4)	412 (4)	−8 (11)
H(14)	−6 (4)	476 (3)	238 (9)	H(29)	278 (4)	377 (4)	763 (11)
H(15)	274 (3)	87 (3)	−230 (8)	H(30)	329 (4)	329 (4)	704 (10)

In order to determine the absolute configuration, equi-inclination Weissenberg photographs were taken of the zero to third layer lines around the a and b axes with Cu $K\alpha$ radiation. Some of the calculated intensities and observed relations between hkl and its counter reflexion $hk\bar{l}$ are compared in Table 1. The agreement in the table indicates that the absolute configurations of the complex anion and cation are those illustrated in Figs. 2 and 3 respectively. The complex cation, $(-)_{589}$-[Co(ox)(en)$_2$]$^+$, has the absolute configuration $\varDelta(\delta\lambda)$, in agreement with the result of Aoki, Matsumoto, Ooi & Kuroya (1973). The final atomic parameters are tabulated in Table 2, together with their estimated standard deviations.*

Description of the structure and discussion

The crystal is ionic, comprising [Co(ox)(en)$_2$]$^+$, [Co(CN)$_2$(mal)(NH$_3$)$_2$]$^-$ and water molecules. In Fig. 1 is shown a projection of the structure along c. Perspective drawings of the complex anion and cation are given in Figs. 2 and 3 respectively. They correctly represent the absolute configurations. In the complex anion the Co atom is surrounded nearly octahedrally by two O atoms of the malonato group, two N atoms of ammonia molecules, and two C atoms of cyano groups. The two ammonia molecules and two cyano groups are both in *cis* positions. The conformation of the malonato–cobalt ring assumes a boat conformation, in agreement with that reported for Na($+$)$_{589}$-[Co(mal)$_2$-(en)].2H$_2$O (Butler & Snow, 1971). It differs, however, from that reported for $(-)_{589}$-[Co(NO$_2$)$_2$(en)$_2$] $(+)_{589}$-[Co(mal)$_2$(en)] where the six-membered chelate rings

___

* A list of structure factors has been deposited with the British Library Lending Division as Supplementary Publication No. SUP 32242 (20 pp.). Copies may be obtained through The Executive Secretary, International Union of Crystallography, 13 White Friars, Chester CH1 1NZ, England.
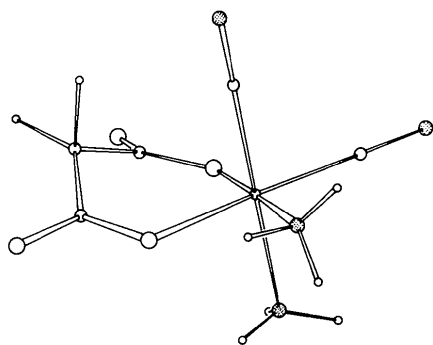
adopt a flattened conformation (Matsumoto & Kuroya, 1972), and for $(-)_{589}$-[Co{(-)pn}$_3$] $(+)_{589}$-[Cr(mal)$_3$] where the six-membered chelate rings adopt a flattened-boat conformation (Butler & Snow, 1976). The conformation of this six-membered chelate ring is thus highly dependent on its environment as predicted by Butler & Snow (1976). The geometries of the cyano groups and ammonia molecules are the same as those observed in other related complexes. Bond distances and angles within the complex ions are listed in Table 3.

The geometry of the complex cation is very similar to those reported by Aoki *et al.* (1973). The C(1)–C(2) distance, 1·556 (6) Å, is slightly longer than the normal $C(sp^2)$–$C(sp^2)$ distance, in agreement with that reported by them. Other bond distances and angles are normal, as listed in Table 3.

The packing of the complex cations, anions, and water molecules is illustrated in the projection down c in Fig. 1, where the hydrogen bonds are indicated by broken lines. The hydrogen-bond distances are listed in Table 4. The complex cations, anions, and water molecules form a three-dimensional network of hydrogen bonds, and all of the N and O atoms participate in the hydrogen-bonding. The water molecules are arranged around the screw diads and they are held together by hydrogen bonds forming a helical structure along c.

An aqueous solution of K($+$)$_{589}$-[Co(CN)$_2$(mal)-(NH$_3$)$_2$] gives a CD peak showing three components in the region of the first absorption band (Ito & Shibata, 1976). The optical activity of this complex anion arises from the chiral coordination of the four monodentates: two cyano groups and two ammonia groups. An appropriate designation of the absolute configuration of this type of complex has not yet been established. The absolute configuration of the complex anion can be designated as skew-pairs $\varDelta$, provided that the chirality is defined by the line joining the two C atoms of the cyano groups and that joining the two N atoms of the ammonia molecules.

Fig. 2. A perspective drawing of the complex anion $(+)_{589}$-[Co(CN)$_2$(mal)(NH$_3$)$_2$]$^-$.

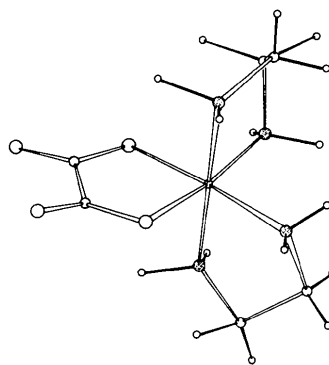Fig. 3. A perspective drawing of the complex cation $(-)_{589}$-[Co(ox)(en)$_2$]$^+$.

The change of the observed intensities by X-irradiation

It appeared that the change of the observed intensities could be ascribed to the change in the secondary extinction effect. The crystal easily loses water of crystallization and it was thought that the change might be related to the water content of the crystal. In order to confirm this point, the following 14 reflexions were carefully selected and the time dependence of the intensities was measured under continuous X-irradiation: (i) seven very strong, low-angle reflexions for which the contribution of water molecules to the structure amplitudes is less than 12%; (ii) four reflexions of medium intensity with 2θ in the range 17–33° of which the intensities were little affected by irradiation; this is to check the electronic circuitry and crystal stability during the period of the measurement; (iii) three reflexions of which the intensities are very sensitive to the loss of water molecules. Actually the contribution of water molecules to these structure amplitudes is more than 80%. The intensity measurement was carried out on a manual four-circle diffractometer using Mo $K\alpha$ radiation monochromated by a graphite plate. A crystal was sealed in a thin-walled Lindemann-glass capillary together with a small piece of wet filter paper. The X-ray tube was operated under usual working conditions and the crystal specimen was irradiated. The intensities

Table 3. *Bond distances (Å) and angles (°) with their estimated standard deviations*

Co(1)–O(1)	1·921 (3)	Co(2)–C(7)	1·876 (5)
Co(1)–O(2)	1·903 (3)	Co(2)–C(8)	1·900 (5)
Co(1)–N(1)	1·962 (4)	Co(2)–O(5)	1·920 (3)
Co(1)–N(2)	1·946 (4)	Co(2)–O(6)	1·932 (3)
Co(1)–N(3)	1·954 (4)	Co(2)–N(7)	1·952 (4)
Co(1)–N(4)	1·951 (4)	Co(2)–N(8)	1·993 (4)
O(1)–C(1)	1·276 (5)	C(7)–N(5)	1·136 (7)
O(2)–C(2)	1·282 (5)	C(8)–N(6)	1·127 (7)
C(1)–C(2)	1·556 (6)		
C(1)–O(3)	1·222 (6)	O(5)–C(9)	1·277 (5)
C(2)–O(4)	1·239 (6)	O(6)–C(11)	1·267 (6)
		C(9)–C(10)	1·535 (6)
N(1)–C(3)	1·484 (7)	C(11)–C(10)	1·519 (7)
N(2)–C(4)	1·484 (6)	C(9)–O(7)	1·234 (5)
N(3)–C(5)	1·479 (6)	C(11)–O(8)	1·247 (6)
N(4)–C(6)	1·483 (6)		
C(3)–C(4)	1·522 (7)		
C(5)–C(6)	1·516 (7)		

O(1)–Co(1)–O(2)	86·3 (1)	C(7)–Co(2)–C(8)	86·3 (2)
N(1)–Co(1)–N(2)	86·0 (2)	O(5)–Co(2)–O(6)	92·5 (1)
N(3)–Co(1)–N(4)	86·1 (2)	N(7)–Co(2)–N(8)	91·8 (2)
		C(7)–Co(2)–O(5)	91·1 (2)
Co(1)–O(1)–C(1)	112·4 (3)	C(8)–Co(2)–O(5)	91·1 (2)
Co(1)–O(2)–C(2)	112·1 (3)	C(8)–Co(2)–O(6)	94·1 (2)
O(1)–C(1)–C(2)	113·6 (4)	C(7)–Co(2)–N(7)	90·4 (2)
O(2)–C(2)–C(1)	115·0 (4)	C(7)–Co(2)–N(8)	92·0 (2)
O(1)–C(1)–O(3)	125·5 (4)	C(8)–Co(2)–N(7)	91·3 (2)
O(2)–C(2)–O(4)	124·4 (4)	O(5)–Co(2)–N(8)	85·9 (2)
		O(6)–Co(2)–N(7)	86·0 (2)
Co(1)–N(1)–C(3)	109·4 (3)	O(6)–Co(2)–N(8)	87·8 (2)
Co(1)–N(2)–C(4)	108·8 (3)		
N(1)–C(3)–C(4)	106·9 (4)	Co2–O(5)–C(9)	126·0 (3)
N(2)–C(4)–C(3)	105·9 (4)	Co(2)–O(6)–C(11)	125·4 (3)
Co(1)–N(3)–C(5)	108·7 (3)	O(5)–C(9)–C(10)	119·8 (4)
Co(1)–N(4)–C(6)	109·5 (3)	O(6)–C(11)–C(10)	120·8 (4)
N(3)–C(5)–C(6)	107·1 (4)	C(9)–C(10)–C(11)	116·7 (4)
N(4)–C(6)–C(5)	106·4 (4)	O(5)–C(9)–O(7)	121·3 (4)
		O(6)–C(11)–O(8)	119·9 (4)
		Co(2)–C(7)–N(5)	177·1 (4)
		Co(2)–C(8)–N(6)	177·5 (5)

Table 4. *Hydrogen-bond distances (Å) with their estimated standard deviations*

Key to symmetry operations

(i)	x,	y,	z
(ii)	x,	y,	$-1·0 + z$
(iii)	$0·5 + x$,	$0·5 - y$,	$1·0 - z$
(iv)	$-x$,	$0·5 + y$,	$0·5 - z$
(v)	$-x$,	$-0·5 + y$,	$0·5 - z$
(vi)	$0·5 - x$,	$1·0 - y$,	$0·5 + z$
(vii)	$0·5 - x$,	$1·0 - y$,	$-0·5 + z$

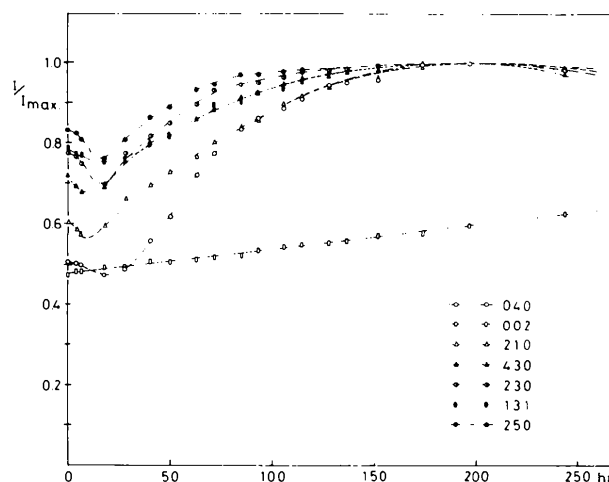|			
N(1)···O(7^v)	2·981 (5)	N(2)···O(4^{ii})	2·808 (5)
N(2)···O(w2^i)	3·101 (5)	N(3)···O(6^i)	3·048 (5)
N(3)···O(8^i)	3·157 (6)	N(3)···N(6^{ii})	3·003 (6)
N(4)···O(3^{ii})	2·909 (5)	N(4)···O(4^{ii})	3·108 (5)
N(4)···O(5^v)	3·001 (4)	N(7)···O(2^i)	3·184 (5)
N(7)···O(w2^i)	3·191 (7)	N(7)···O(w3^i)	2·934 (6)
N(8)···O(1^{iv})	3·174 (6)	N(8)···O(w1^i)	2·953 (7)
O(w1)···N(5^{ii})	3·022 (8)	O(w2)···N(5^{vii})	2·875 (6)
O(w2)···O(w1^i)	2·763 (6)	O(w2)···O(w3^{ii})	2·955 (7)
O(w3)···O(8^{iii})	2·688 (6)	O(w3)···O(w1^{vi})	2·789 (7)

Fig. 4. Time dependence of I/I_{max} of some strong, low-angle reflexions belonging to category (i).

Table 5. *Intensity changes in some strong, low-angle reflexions*

h k l	2θ	I_{init}	I_{max}	I_{calc}	I_{init}/I_{max}
0 4 0	8·99	2509 (17)	4957 (17)	5116	0·506 (4)
0 0 2	10·77	2335 (16)	4930*	4930	0·474
2 1 0	5·35	2478 (17)	4103 (21)	4424	0·604 (5)
4 3 0	11·84	1602 (11)	2214 (12)	2172	0·724 (6)
2 3 0	8·31	1526 (11)	1968 (12)	1967	0·775 (7)
1 3 1	8·95	1413 (10)	1795 (11)	1873	0·787 (7)
2 5 0	12·25	1028 (9)	1232 (10)	1142	0·834 (10)

* The maximum intensity is replaced by the calculated value.

Table 6. *Time dependence of the intensities of reflexions belonging to categories* (ii) *and* (iii)

Index Category $2\theta(°)$ X-irradiation time (h)	710 (ii) 17·22	771 (ii) 23·94	10,4,2 (ii) 28·35	136 (ii) 33·50	060 (iii) 13·50	350 (iii) 13·41	401 (iii) 11·14
0·0	281 (2)	232 (1)	148 (1)	93 (1)	39 (1)	91 (1)	147 (1)
3·9	281	228	148	94	39	91	146
6·6	278	229	147	96	39	93	149
17·8	282	230	147	95	40	92	147
27·8	282	232	147	96	39	91	148
40·3	281	235	147	94	39	92	147
50·0	283	233	147	95	41	91	146
62·9	283	235	146	94	40	92	147
71·6	285	236	146	96	40	94	147
84·7	283	235	149	95	38	93	145
92·8	285	236	147	94	39	92	146
105·4	281	236	146	94	39	92	144
114·5	282	237	146	96	39	93	144
127·5	283	237	146	94	39	92	144
136·7	283	238	146	94	39	92	143
151·4	281	238	145	94	39	91	143
173·6	281	235	143	95	39	91	143
196·4	284	235	145	92	38	91	141
243·0	278	234	142	92	37	91	138

of the 14 selected reflexions were measured at an appropriate time interval. The measurement was carried out with the $\omega-2\theta$ scan technique at a scan rate of 1° min^{-1} in ω.

The results are shown in Fig. 4 and Tables 5 and 6. The intensities of the seven reflexions of category (i) increased slowly during the period of the measurement in the same way as observed in the case of data set 1, however, those of categories (ii) and (iii) changed little in intensity. All the intensities, except 002, saturated simultaneously after 200 h, but the 002 still increased. In Table 5, the initial and maximum intensities of very strong, low-angle reflexions of category (i) are compared with their calculated values. For 002, the maximum intensity is replaced by the calculated value, because the intensity of 002 increased linearly and the saturation of the intensity may be expected to take place after a long irradiation. The observed intensities of seven very strong, low-angle reflexions increased

with time and approached the calculated values. The agreement between the maximum intensities and the calculated intensities is fairly good, as shown in Table 5. Moreover, the larger the intensity is, the larger is the change in the observed intensity. Accordingly this phenomenon may be ascribed to the change in the secondary extinction effect. This conclusion may be supported by the unchanged intensities of the other seven reflexions of categories (ii) and (iii) with irradiation times, as shown in Table 6. The constant intensities of four reflexions of category (ii) and three reflexions of (iii) may indicate that appreciable structural change in the crystal did not occur. The secondary extinction factor, y, is related to the diffracting power of the crystal, and the stronger the diffracted intensity is, the smaller is the value of y (Zachariasen, 1967). The value of I_{init}/I_{max} is assumed to be equal to the value of y in the initial state of the crystal. As can be seen from Table 5, a small value of y is always associated with

strong reflexion (I_{max}). This trend strongly supports the intensity change being due to the secondary extinction effect.

In Fig. 4, for each strong, low-angle reflexion of category (i), the value of I/I_{max} corresponding to the value of the extinction factor is plotted as a function of irradiation time. The time dependence of I/I_{max} differs from reflexion to reflexion; in particular, 002 increases linearly with time and shows no saturation. The rates of change of I/I_{max} with irradiation time are similar if the reciprocal-lattice points lie close to each other; for example, 040, 230 and 250 behave similarly and so do 210 and 430. In addition, the rate of change of 131 is intermediate between 002 and other reflexions. This seems to indicate an anisotropic change in the extinction effect.

The change in the extinction effect may be caused by a small loss of water molecules under irradiation. As can be seen from Fig. 1, the water molecules are enclosed in a channel parallel to c, forming a helical structure around a screw diad. The water molecules are weakly hydrogen-bonded to the N and O atoms of the complex ions forming the wall of the channel. Such a structure suggests that the water molecules can easily come out of the channel. In fact, a crystal specimen not sealed in a glass capillary showed different unit-cell dimensions after one day: $a' = 16.092 (-0.617)$, $b' = 18.001 (-0.138)$, $c' = 7.610 (+0.041)$ Å. Such contraction in the a and b directions and elongation along c may reasonably correspond to the loss of water molecules from the channels parallel to c. The small change

of cell dimension along c may be related to the slow change in the extinction effect of 002.

The observed intensities of very strong, low-angle reflexions of category (i), except 002, decreased slowly with irradiation time until 20 h and then began to increase. This change cannot be accounted for.

References

AOKI, T., MATSUMOTO, K., OOI, S. & KUROYA, H. (1973). *Bull. Chem. Soc. Japan*, **46**, 159–162.

BUTLER, K. R. & SNOW, M. R. (1971). *Chem. Commun.* pp. 550–551.

BUTLER, K. R. & SNOW, M. R. (1976). *J. Chem. Soc. Dalton*, pp. 251–258.

International Tables for X-ray Crystallography (1962). Vol. III. Birmingham: Kynoch Press.

ITO, T. & SHIBATA, M. (1976). *Inorg. Chem.* In the press.

MATSUMOTO, K. & KUROYA, H. (1972). *Bull. Chem. Soc. Japan*, **45**, 1755–1759.

SHINTANI, H., SATO, S. & SAITO, Y. (1976). *Acta Cryst.* B**32**, 1184–1188.

STEWART, R. F., DAVIDSON, E. R. & SIMPSON, W. T. (1965). *J. Chem. Phys.* **42**, 3175–3187.

ZACHARIASEN, W. H. (1967). *Acta Cryst.* **23**, 558–564.

The Crystal Structures of Two Enol Acetates

BY ARNAUD DUCRUIX AND CLAUDINE PASCARD-BILLY

Institut de Chimie des Substances Naturelles, Laboratoire de Cristallochimie, CNRS, 91190 Gif/Yvette, France

The crystal structures of 1-*O*-acetyl-2,3:4,5-di-*O*-isopropylidene-δ-*erythro*-pent-1-enitol and of the corresponding *threo* compound (C$_{13}$H$_{20}$O$_6$) were solved by application of the phase function. Crystals of the *erythro* compound are monoclinic, $a = 5.435$ (2), $b = 14.703$ (6), $c = 9.332$ (4) Å, $\beta = 104.15$ (9)°, $Z = 2$, space group *P*2$_1$. The *threo* crystals are orthorhombic, space group *P*2$_1$2$_1$2$_1$, $a = 5.543$ (2), $b = 8.240$ (3), $c = 32.336$ (10) Å, $Z = 4$. Intensities were collected on a four-circle diffractometer with Cu *K*α radiation. The final *R* values are 0.04 for the *erythro* compound and 0.05 for the *threo*. In both structures the stereochemistry about the double bond is *Z*.

Introduction

In the course of a general study of the acyclic sugar derivatives (Ducruix & Pascard-Billy, 1974, 1975a,b)

and in collaboration with Professor Horton's Laboratory, we have undertaken the determination of the crystal structures of two enol acetates. The aim was to assign a precise geometry at the double bond